

COMPARISON OF PARTIAL DISCHARGE CHARACTERISTICS FROM INSULATION DEFECTS IN 11KV EPR CABLE

A. J. Reid^{1*}, X. Peng², X. Hu¹, M. D. Judd¹, W. H. Siew¹, C. Zhou² and D. M. Hepburn²

¹University of Strathclyde, Glasgow, UK

²Glasgow Caledonian University, Glasgow, UK

*Email: alistair.reid@eee.strath.ac.uk

Abstract: This paper presents a study on the identification and classification of PD patterns produced by various defect topologies in MV cable. Laboratory-based measurements are first described, with a number of well-defined defects having been introduced into various cable samples. Five defects have been considered; void, protrusion on the outer conductor, floating protrusion, breach in the outer conductor, and surface discharges at the end terminations. Characteristic phase-resolved patterns are evident for each defect type. Features such as the number of pulses per half cycle, pulse amplitude and phase position can be correlated to the type and severity of the defect. The floating protrusion defect was found to present the highest risk of failure under the experimental conditions outlined. Automated defect classification of the five geometries was also considered using parameters of the individual PD pulse shapes. This approach circumvents the requirement of a phase-reference, which is often difficult to obtain on-site. Features such as the rise time, standard deviation, skewness and kurtosis of the pulses were extracted. Of the data collected, around 90% of pulses could be positively identified as originating from the correct PD source, based on analysis of pulse shape.

1 INTRODUCTION

Electrical power distribution relies heavily on a vast network of medium voltage (MV) underground cables for local power delivery. In the UK, the vast majority of these cable networks were installed in the 1950's and 1960's [1]. Given that the expected design life of these assets is in the order of 60-70 years [2,3], together with the increasing frequency of observed failures, it is clear that cable replacement strategies will pose a significant challenge over the coming decades. One UK distribution network operator has reported that the replacement cost of their 11kV and 6.6kV cable network is in the order of around \$7 billion, and at the current replacement rate, would take 700 years to complete [4]. Condition monitoring technologies have, therefore, recently played a considerably greater role in attempting to target cables that pose the most urgent short-term reliability concerns. On-line monitoring is advantageous in that repetitive measurements can facilitate trending analysis and correlation with external factors such as thermal stress, load, humidity or mechanical stress [5-9]. Although large volumes of data can be collected, these are often difficult to interpret in terms of the original PD mechanism or source. The ability to relate characteristic phase-resolved patterns or pulse shapes to a particular PD source or mechanism is advantageous for more effective diagnosis but is difficult in practice due to the necessity of isolating the fault, removing it, and making a detailed analysis of the internal structure. Most structural faults which cause PD are damaged beyond recognition prior to identification and replacement. The complexity is increased when we consider that characteristic phase-

resolved data is often produced by multiple concurrent defects as well as external interference. To produce distinctive, separable PD characteristics, a number of PD sources were introduced artificially into PD-free ethylene-propylene rubber (EPR) cable samples. In this way the geometry of the defect was known, and could be related to the resultant output signals. It was also necessary ensure that end terminations were PD-free so that measured signals were known to originate from a single source.

1.1 Partial discharge sources

PD in shielded power cable falls into two categories; internal or external. Within the extruded dielectric, e.g. EPR or cross-linked polyethylene (XLPE), internal PD may occur due to manufacturing defects, damage during installation, or faults generated by the inherent working stresses in the cable. Common defect sources are reported in [10]. This study focuses on PD in EPR insulated cables designed to operate at 11 kV. Five common faults were investigated as discussed below.

In both XLPE and EPR insulated systems, the possibility of void formation exists during and immediately after the curing phase of cable manufacture, since the products of peroxide decomposition, commonly found in cable formation, are gaseous at high temperature and attempt to escape the insulation during depressurisation [11]. The void was therefore chosen as a PD source. Voids of known dimensions were introduced artificially by drilling cylindrical cavities in the insulation layer directed radially from the outer to inner conductors. The

second type of defect considered was a protrusion occurring on a conductor, which may also occur due to a manufacturing defect or due to external damage. Protrusions may occur on the inner or outer conductors, producing a strongly inhomogeneous localised field. The third defect considered was a protrusion, which, not being connected to the inner or outer conductors, is floating. The fourth fault considered is delamination, or an interruption in the semiconducting layer or conductor. The fifth defect considered is an end termination discharge, which may occur in the absence of stress cones, or due to their incorrect installation. Provided a sufficient gap exists between the inner and outer conductors at the end termination, the likelihood of breakdown is less than that of the internal PD types described previously. All five defect topologies are illustrated in Figure 1.

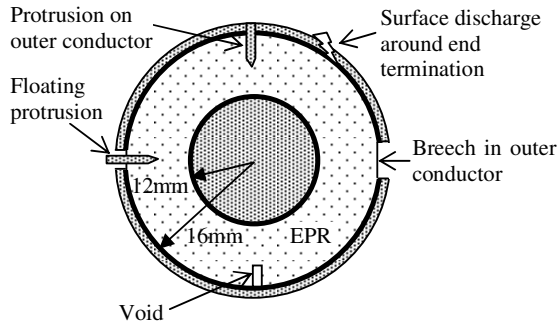


Figure 1: Illustration of defects introduced into the cable samples individually. Geometries are as follows: Type 1 - Surface discharge around end termination, Type 2 - Void (2 mm depth with 0.4 mm diameter), Type 3 - Floating protrusion (2 mm depth into insulation layer with 0.4 mm diameter), Type 4 - Protrusion on outer conductor (2 mm depth into insulation layer with 0.4 mm diameter), Type 5 - Breach in outer conductor (7 mm x 7 mm).

2 METHODOLOGY

The experimental setup is shown in Figure 2. PD-free single-phase cable samples of 1.5 m - 2 m in length were initially connected to the high voltage supply and tested for intrinsic PD. The outer conductors of the samples were connected to earth at both ends. Each sample was terminated at both ends using pre-moulded stress cones, and tested up to 13 kV. Intrinsic PD was found to be below 2pC, corresponding to the background noise level of the measurement system. Defects were subsequently introduced into the samples. A high-frequency current transformer (HFCT) was placed around one of the cable's earth straps and its output was measured concurrently with the phase reference and IEC60270 waveforms using a 1 GHz LeCroy 104Xi oscilloscope. The applied voltage was increased from inception to $1.2 U_0$ (13kV) in steps of 1 kV, with 50 phase-resolved PD traces recorded for each voltage. All data was recorded

using a 2 ms time base and a sampling rate of 100 MSs^{-1} which was sufficient to capture the detail of the individual pulse shapes, along with their phase position relative to the AC reference wave.

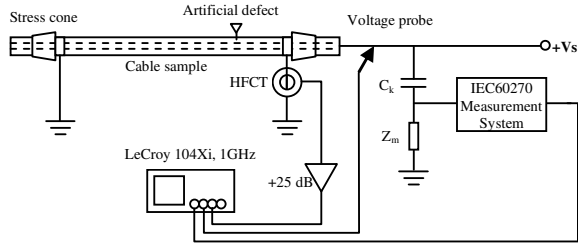


Figure 2: Experimental setup. PD was measured simultaneously using an HFCT and an IEC60270 system. Data was measured relative to the 50 Hz AC supply. C_k represents the IEC coupling capacitor and Z_m the measurement impedance.

The frequency response of the HFCT used in this investigation is shown in Figure 3. The graph was obtained by comparing the frequency spectra of an injected fast transient current pulse with that of the corresponding HFCT output. The sensitivity is around 4 V/A in the range 5 kHz - 10 MHz. The peak at 50 MHz is an artefact of the test setup, caused by resonance in the measurement circuit.

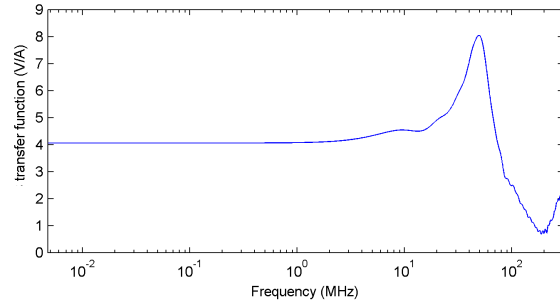


Figure 3: Frequency response of the HFCT.

For comparison, PD was measured concurrently using an LDIC LDS-6 IEC60270 measurement system [12]. This allowed the accuracy of phase resolved partial discharge (PRPD) data to be confirmed. For subsequent PRPD pattern and PD pulse shape analysis, only HFCT measurements were considered. For HFCT measurements, a 50 Ω oscilloscope input impedance was used. For on-site PD location on a cable system, it is often recommended that an input impedance of 1 M Ω is used as this provides a higher sensitivity due to the effective open-circuit load impedance in comparison with the 50 Ω cable impedance. However, while effectively doubling the measured voltage, the impedance mismatch distorts the true PD pulse shape due to the presence of multiple pulse reflections along the connecting cable. Since this study is concerned with phase-resolved data and accurate characterisation of pulse shape,

higher sensitivity was sacrificed in favour of measurement accuracy.

3 RESULTS

3.1 Phase resolved data

Figure 4 shows phase-resolved PD plots for the five defects considered. PD characteristics are evident in features such as the number of pulses per half-cycle, pulse amplitude, and phase position. 50 traces were captured for each applied voltage. 10 phase cycles have been superimposed for each defect. Valuable discriminatory information can be gathered by examining both single-cycle phase-related data and data collated over a longer period. For example, in the case of the void data in Figure 4(a), examination of one cycle reveals that two to three pulses typically appear in the first and third quadrants. Plotting over a longer period reveals that pulses are confined to six phase ranges, leading to the appearance of six clusters of data. The highest pulse amplitudes occur in the 55° - 65° range.

Figure 4(b) shows a PRPD plot for a protrusion on the outer conductor. A single pulse usually occurs per half cycle in each phase window, resulting in two single clusters appear in the ranges 35° - 70° and 200° - 250° . An increase in electric field stress (applied voltage) is accompanied by a decrease in pulse amplitude, as shown in Figure 4(c).

Referring to Figure 4(d), which shows the PRPD pattern for a floating protrusion, one PD pulse occurs per half cycle. Maximum PD amplitude at operational voltage is lower than that of the protrusion on the outer conductor (75 mV compared with 250 mV). As the applied voltage is increased, PD magnitude decreases to almost zero and the cable eventually breaks down at 13 kV. This is indicative of the severity of the defect. Since the protrusion is not electrically connected to any part of the sample, charge accumulation results, eventually reaching a value sufficient to bridge the insulation.

The breach on outer conductor is characterised by low amplitude PD pulses of around 20 mV peak amplitude occurring in two clusters in the ranges 45° - 110° and 200° - 275° as shown in Figure 4(e).

End termination discharges, shown in Figure 4(f), are characterised by high amplitude pulses (up to 2000 mV peak) in the negative half cycle, coupled with a high repetition rate, with several hundred pulses occurring in a single phase cycle. In this case the outer conductor and semiconducting layers have been stripped back from the end terminations, with no stress cones installed. A high electric field concentration is present around the terminated edge of the outer conductor and

semiconductors. Despite the high PD pulse amplitude, the defect does not present an immediate risk of breakdown since discharges are external and a sufficient path length exists between the terminated ends of the inner and outer conductors to prevent external tracking.

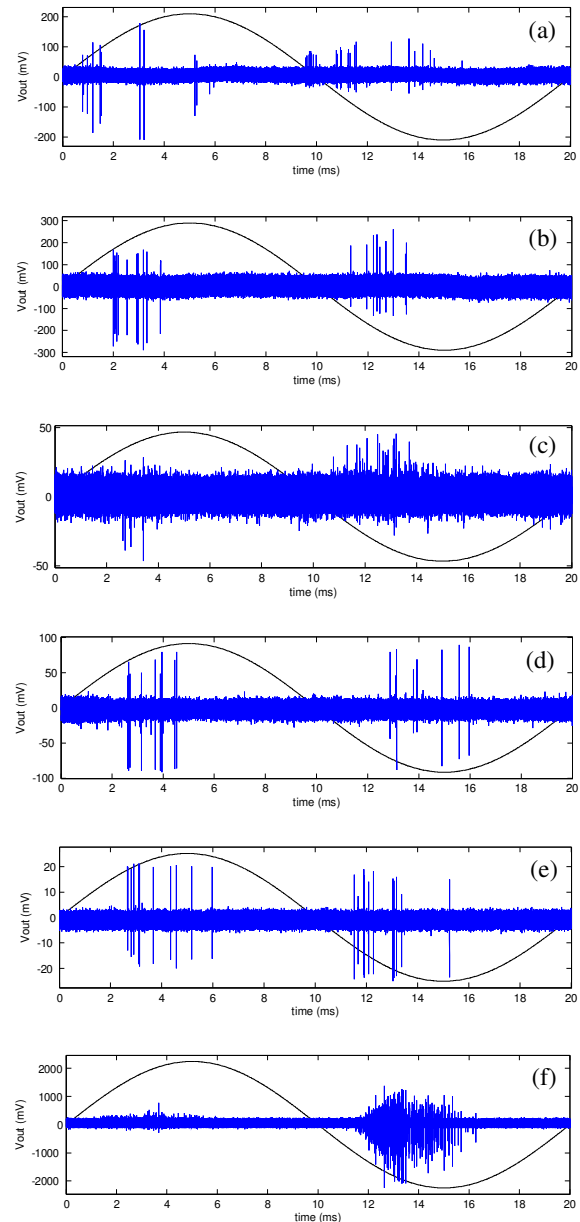


Figure 4: PRPD plot for (a) void of 2mm depth and 0.4 mm diameter, 11 kV (b) 2mm protrusion on the outer conductor, 11 kV, (c) 2mm protrusion on the outer conductor, 12 kV (d) floating protrusion inserted 2mm from the surface of the EPR insulation layer, 11 kV, (e) 7 mm x 7 mm breach on the outer conductor and outer semiconducting layers, 11 kV, (f) discharges occurring due to high electric field stressing on the end terminations, 11kV.

3.2 PD classification

The development of automated PD classification algorithms has been well documented [13-15]. Conventionally, statistical features of phase-resolved patterns have been extracted for this purpose. Identification of a unique PD source or mechanism often involves identification of a cluster when two features of a chosen data set are plotted against one another. Since it is often difficult to obtain a reliable phase reference on-site, it is proposed that a number of features may be extracted from the individual PD pulses without correlation to the phase reference. The effectiveness of classification, based on these time-domain features alone, was examined.

The signal classification process is illustrated in Figure 5. Firstly, data denoising and signal reconstruction was applied. Secondly, a data denoising algorithm based on the Second Generation Wavelet Transform [16] was applied. Signal classification and signal type judgment, based on the chosen PD parameters, was then applied to classify data into either PD signals or interference signals. Meanwhile, PD and interference signal parameters were stored for subsequent comparison with new PD data in order to effectively classify signals into known types.

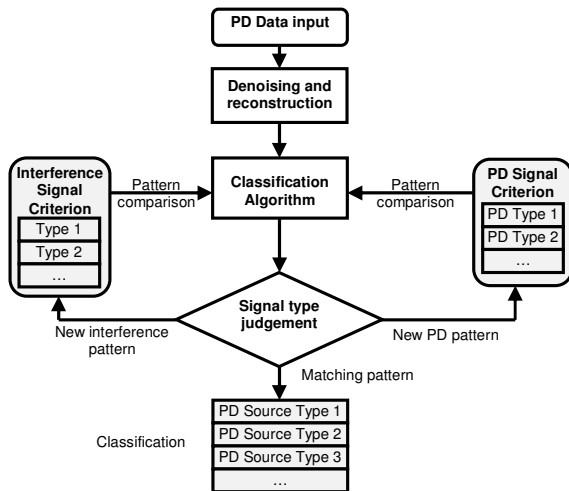


Figure 5: Flow chart of signal classification.

In this case, PD parameters were pulse width, rise time, standard deviation, skewness, kurtosis, crest factor (maximum magnitude divided by root mean square magnitude), form factor (root mean square magnitude divided by average value), equivalent time length (T) and equivalent band width (W) [17].

Typical PD pulses produced by the five defect topologies examined are illustrated in Figure 6. Features extracted from each of these individual pulses are listed in Table 1 for comparative purposes.

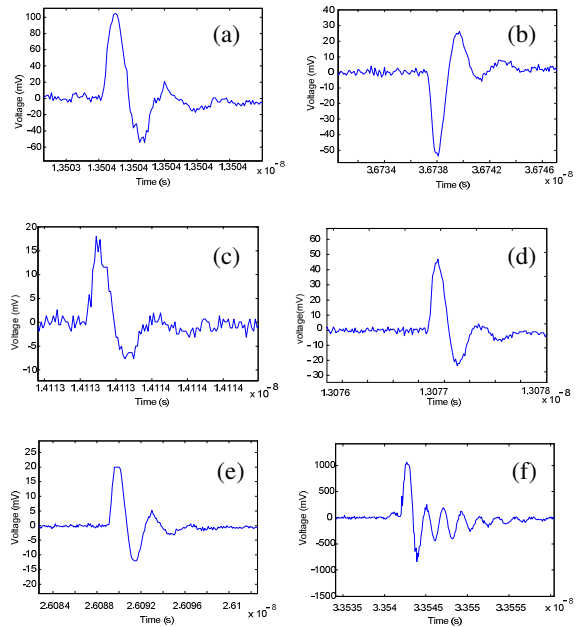


Figure 6: PD pulse from a (a) 2mm void, 11 kV, (b) 2mm protrusion on the outer conductor, 11 kV, (c) 2mm protrusion on the outer conductor, 12 kV, (d) floating protrusion, 11 kV, (e) breach in the outer conductor, 11 kV, (f) surface discharge on the end termination, 11 kV.

Table 1: Extracted features from the 6 example PD pulses shown in Figure 10.

| | Void | Protrusion | Floating protrusion | Outer conductor breach | End termination discharge |
|------------------------|-------|------------|---------------------|------------------------|---------------------------|
| Pulse width (ns) | 160 | 150 | 170 | 160 | 140 |
| Rise time (ns) | 70 | 70 | 80 | 40 | 60 |
| Standard deviation | 35 | 18 | 9 | 7 | 396 |
| Skewness | -0.40 | 0.30 | 0.26 | -0.48 | -0.58 |
| Kurtosis | 1.75 | 1.65 | 1.52 | 1.73 | 1.79 |
| Crest factor | 1.45 | 1.45 | 1.51 | 1.29 | 1.37 |
| Form factor | 1.14 | -1.16 | -1.19 | 1.14 | 1.15 |
| Equivalent time length | 8.28 | 6.83 | 7.98 | 8.53 | 6.76 |
| Equivalent band width | 8.90 | 8.95 | 13.5 | 10.19 | 8.30 |

Examples of PD classification applied to three data sets are shown in Figure 7. The figure shows three typical phase cycles from the end termination discharge. One PD signal type, plotted in red, is extracted from the raw data through analysis and classification of the pulse shape. End termination discharges are classified as type 1 in the majority of cases. Some erroneous classifications occasionally occur, as illustrated in Figures 7(b) and (c), where discharges have been classified as type 2, (shown in green). For the measured data on all defect sources, overall PD classification accuracy based on pulse shape was around 90%.

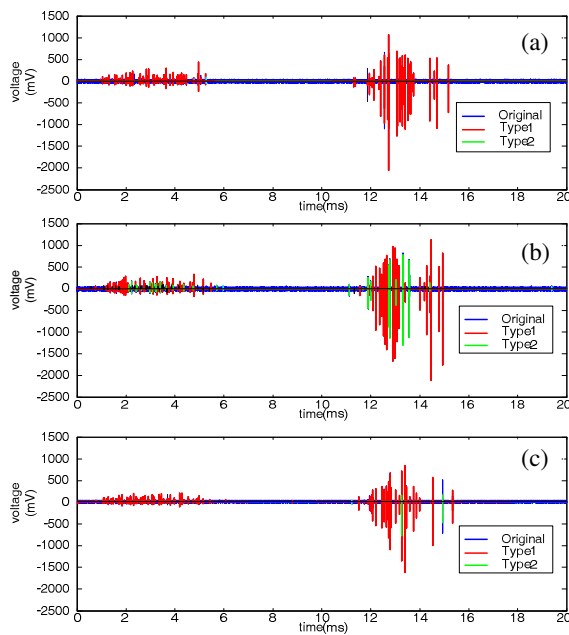


Figure 7: PD signal classification for three example measurements of PRPD data for the end termination discharge source. 1 phase cycle. 11kV. Correct classifications shown as 'Type 1', erroneous classifications as 'Type 2'.

4 DISCUSSION

PD feature extraction based on parameters of the individual pulse shapes has shown potential to provide positive identification of a number of common defect configurations introduced artificially into an 11 kV MV cable sample. Although classification accuracy is high for certain configurations, this, or any other individual technique is unlikely to identify all defects with 100% accuracy. It is therefore proposed that a combined approach to feature extraction is necessary, including raw PD signal analysis, phase-resolved pattern analysis and mapping of the equivalent time length and equivalent bandwidth (T-W mapping) [16].

Short cable samples of around 1.5 m in length were used in this investigation. For cable systems in which the PD source occurs a significant distance from the sensor, characterisation based on pulse shape is likely to be less effective, with the boundaries between pulse parameters blurred by the effects of dispersion and by the low-pass characteristics of the cable. For measurement of localised PD events, such as those occurring in MV switchgear systems, a more significant variation in pulse shapes between the defect geometries considered may occur, leading to defect separation more closely approaching that of the laboratory-based results presented in this study.

Regarding the phase-resolved measurement results presented in section 3.1, it is noted that correlation with on-site data will be often difficult, given the frequent lack of a phase reference. A novel approach to this problem, where the phase angle is plotted in polar form on a relative scale, rather than in terms of an absolute value, will be discussed in future.

5 CONCLUSIONS

A range of defect geometries encountered in 11 kV MV EPR cable have been studied under laboratory conditions and characterised in terms of phase-resolved patterns and individual pulse shapes. Five defect topologies were considered; void, protrusion on the outer conductor, floating protrusion, breach in the outer conductor, and surface discharges at the end terminations. The floating protrusion was found to present the highest risk of failure. Automated defect classification of the five geometries was considered based on features of the individual pulse shapes. It was found that 90% of pulses could be positively identified in the cases considered. It is proposed that greater classification accuracy can be achieved by combining analysis of the raw PD pulses with other techniques such as phase-resolved pattern analysis and T-W mapping.

6 ACKNOWLEDGMENTS

This research is funded by the EPSRC through grants EP/G029210/1 (University of Strathclyde) and EP/G028397/1 (Glasgow Caledonian University). The authors gratefully acknowledge the support of EDF Energy and Prysmian Cables and Systems Ltd.

7 REFERENCES

- [1] L. Renforth, C. Smith, R. MacKinlay, and C. Walton. An integrated approach to on-line PD monitoring and diagnosis of MV plant condition for application as a pre-maintenance tool. In Proc. 17th International Conference on Electricity Distribution (CIRED), Barcelona, Spain, May 2003.
- [2] L. Renforth, R. Mackinlay, and M. Michel. MV cable diagnostics - applying online PD testing and monitoring. In Proc. MNC-CIRED Asia Pacific Conference on MV Power Cable Technologies, September 2005.
- [3] C. Walton and R. Mackinley. PD monitoring: A critical tool for condition-based assessments. *Transmission and distribution world*, pages 38-46, Dec 2003.
- [4] M. Michel. Comparison of off-line and on-line partial discharge MV cable mapping techniques. In Proc. 18th International

- Conference and Exhibition on Electricity Distribution (CIRED), Turin, Italy, June 2005.
- [5] C. Zhou, D. M. Hepburn, M. Michel, X. Song, and G. Zhang. Partial discharge monitoring in medium voltage cables. In Proc. International Conference on Condition Monitoring and Diagnostics, pages 1021--1024, Beijing, China, April 2008.
- [6] H. E. Orton. Diagnostic testing of in-situ power cables: An overview. In Proc. IEEE/PES Asia Pacific Transmission and Distribution Conference and Exhibition, pages 1420-1425, Yokohama, Japan, October 2002.
- [7] S. Boggs and J. Densley. Fundamentals of partial discharge in the context of field cable testing. IEEE Electrical Insulation Magazine, Vol. 16, No. 5, pp. 13-18, Sep/Oct 2000.
- [8] J. C. Chan, P. Duffy, L. J. Hiivala, and J. Wasik. Partial discharge VII: PD testing of solid dielectric cable. IEEE Electrical Insulation Magazine, Vol. 7, No. 5, pp. 9-16, Sep-Oct 1991.
- [9] J. Densley. Ageing mechanisms and diagnostics for power cables: an overview. IEEE Electrical Insulation Magazine, Vol. 17, No. 1, pp. 14-22, Jan-Feb 2001.
- [10] M. S. Mashikian. Preventative maintainable testing of shielded power cable systems. In Proc. Pulp and Paper Industry Technical Conference, pages 59-66, Portland, OR, USA, June 2001.
- [11] M. Brown. Performance of Ethylene-Propylene rubber insulation in medium and high voltage power cable. IEEE Transactions on Power Apparatus and Systems, Vol. 102, No. 2, pages 373-381, February 1983.
- [12] IEC International Standard 60270. High Voltage Test Techniques - Partial Discharge Measurements. International Electrotechnical Commission (IEC), Geneva, Switzerland, 3rd edition, 2000.
- [13] F. H. Kreuger, E. Gulski, and A. Krivda. Classification of partial discharges. IEEE Trans. Electrical Insulation, Vol. 28, No. 6, Pages 917-931, Dec 1993.
- [14] E. Gulski and F. H. Kreuger. Computer-aided recognition of discharge sources. IEEE Trans. Electrical Insulation, Vol. 27, No. 1, pages 82-92, Feb 1992.
- [15] G. C. Stone. Partial discharge diagnostics and electrical equipment insulation condition assessment. IEEE Trans. Dielectrics and Electrical Insulation, Vol. 12, No. 5, pages 891-904, Oct 2005.
- [16] Xiaodi Song, Chengke Zhou, Donald M. Hepburn, Guobin Zhang. Second Generation Wavelet Transform for Data Denoising in PD Measurement, IEEE Transactions on Dielectrics and Electrical Insulation Vol. 14, No. 6, December 2007
- [17] G. C. Montanari and A. Cavallini, A New Approach to Partial Discharge Testing of HV Cable Systems, IEEE Electrical Insulation Magazine, January/February 2006-Vol.22, No.1